

# Determination of Void Shapes, Sizes, Numbers and Locations Inside an Object with Known Surface Temperatures and Heat Fluxes

G. S. Dulikravich and T. J. Martin

Department of Aerospace Engineering, The Pennsylvania State University  
University Park, PA 16802, USA

## Summary

During the past several years we have developed an inverse method that allows a thermal cooling system designer to determine proper sizes, shapes, and locations of coolant fluid passages (holes) in, say, an internally cooled turbine blade. The internally cooled object can be made of materials having distinct thermal diffusivities. Thermal expansion has been neglected although, in principle, it could be included. The result is a simple Laplace's equation for the steady temperature field over a multiply connected domain that is subject to overspecified thermal boundary conditions. This same methodology with minor modifications concerning the type of thermal boundary conditions has been utilized in the nondestructive detection of possible voids in objects with known surface temperature and heat flux distributions.

## Inverse design of coolant flow passages

In the case of an inverse thermal design [1-8], the designer can iteratively enforce a desired heat flux distribution  $q_{out}^{des}$  on the hot outer surface of the blade, while simultaneously satisfying the desired temperature distributions  $T_{out}^{spec}$  on the hot outer surface and specified temperatures  $T_{in}^{spec}$

on the cooled surfaces of each of the holes. This constitutes an over-specified boundary value problem. We can solve the direct Dirichlet problem with the specified temperatures on the inner and outer boundaries for the initially guessed configuration. The temperature field analysis was performed using our boundary integral element code with linearly varying temperature along straight surface panels. Nevertheless, the computed outer surface heat fluxes  $q_{out}^{comp}$  corresponding to the initial guess will not be the same as the desired outer surface heat fluxes  $q_{out}^{des}$ . A properly scaled  $L_2$  norm of the difference between the desired outer surface heat fluxes  $q_{out}^{des}$  and the computed outer surface heat fluxes  $q_{out}^{comp}$  is then minimized by iteratively changing

the sizes, shapes, and locations of the holes. Starting with a large number of guessed holes, all unnecessary coolant passages will eventually be eliminated when their sizes reduce below a prespecified minimal allowable value. This procedure is conceptually similar to optimization of the time evolution of thermal boundary conditions for an object having a fixed geometry and specified time rate of change of temperature throughout the object. For example, this time-dependent inverse problem has been developed for possible application in the optimization of freezing protocols for organs intended for transplant surgery [9]. Minimization of the  $L_2$  norm

was performed automatically using a standard gradient search optimization algorithm of Davidon-Fletcher-Powell [10]. Local minimas in the optimization process were successfully avoided by changing the formulation for the objective function whenever the local minimas were detected [6]. Two definitions of the objective function were used. They represented two different forms of the  $L_2$  norm of the difference between the computed and the desired heat fluxes on the outer surface. Thus, the objective function was either a normalized global error

$$F_1(x) = \frac{\sum_{j=1}^N (q_j^{\text{comp}} - q_j^{\text{des}})^2}{\sum_{j=1}^N (q_j^{\text{des}})^2} \times 100 \quad (1)$$

or a normalized local error at each node

$$F_2(x) = \sum_{j=1}^N \frac{(q_j^{\text{comp}} - q_j^{\text{des}})^2}{(q_j^{\text{des}})^2} \times 100 \quad (2)$$

where the outer boundary was discretized with  $N$  surface panels. Besides minimizing the heat flux error on the outer surface, the final configuration has to satisfy two constraints [4]: a) specified minimum allowable distance between any two holes,  $d^{\text{hole}}$ , having radii  $r_i$  and  $r_k$ , and b) specified minimum allowable distance between any hole and the outer boundary,  $d^{\text{surf}}$ . The two constraints were incorporated into the objective function using a barrier function [10]

$$B(g(x), w_b) = \frac{1}{w_b} \sum_{i=1}^M \left[ \sum_{j=1}^N \frac{d^{\text{surf}}}{(D_j^{\text{surf}} - d^{\text{surf}} - r_i)} + \sum_{k=1}^M \frac{d^{\text{hole}}}{(D_k^{\text{hole}} - d^{\text{hole}} - r_i)} \right] \quad (3)$$

Here,  $M$  is the total number of holes and  $w_b$  is the user specified barrier coefficient which was reduced as the process kept converging. Thus, the composite objective function can have two forms depending on whether the global or local objective function is used for its evaluation.

$$F_m(g(x), w_b) = F_m(x) + B(g(x), w_b) \quad m = 1, 2 \quad (4)$$

In summary, the inverse design protocol consists of the following steps:

- (1) Specify shape of the outer surface and coating of the turbine blade. Also, specify thermal diffusivities of the blade and coating materials.

- (2) Specify temperatures  $T_{in}^{spec}$  and  $T_{out}^{spec}$  on the inner and outer surfaces, respectively.
- (3) Specify the desired heat flux  $q_{out}^{des}$  values on the outer surface.
- (4) Specify manufacturing constraints:
  - (i) minimum distance  $d^{surf}$  between holes and the outer surface,
  - (ii) minimum distance  $d^{hole}$  between any two neighboring holes.
- (5) Specify initial guess for the number of holes,  $M$ , their radii,  $r_i$ , and locations of the centers of the holes,  $x_{ci}$  and  $y_{ci}$ . Thus, there will be  $3 \times M$  design variables if we limit ourselves to circular holes only. Recently [8], we have allowed hole shapes to vary according to a Lamé curve (superelliptic function) expressed as

$$\left(\frac{x - x_{ci}}{a_{ci}}\right)^{n_i} + \left(\frac{y - y_{ci}}{b_{ci}}\right)^{n_i} = 1 \quad (5)$$

Here,  $x_{ci}$  and  $y_{ci}$  are the Cartesian coordinates of the hole center,  $a_{ci}$  and  $b_{ci}$  are the two semi-axis of the hole contour, and the exponent  $n_i$  can vary from  $n_i < 1$  (a four-pointed star), to  $n_i = 1$  (a diamond shape), to  $n_i = 2$  (a circle or an ellipse), to  $n_i \gg 1$  (a square or a rectangle). Moreover, the local  $x, y$  Cartesian coordinate system can be inclined at an arbitrary angle  $\alpha_i$  with respect to the global  $x', y'$  Cartesian coordinate system. Thus, when utilizing Lamé shapes we will have to optimize a total of  $6 \times M$  design variables.

- (6) Using the boundary element method, Laplace's equation for a given multiply connected domain and temperature boundary conditions is solved and heat fluxes  $q_{out}^{comp}$  at the outer boundary are computed.
- (7) Determine relative error between the desired and computed heat fluxes and evaluate the objective function. At the same time the barrier function has to be evaluated to determine the composite objective function  $F_m$ .
- (8) Each of the three (in the case of circular holes) or each of the six (in the case of Lamé shaped holes) design parameters are perturbed by a small amount and steps (6) and (7) are repeated for each perturbation.
- (9) The Davidon-Fletcher-Powell gradient search algorithm [8] is used to find gradient directions for each of the design variables and new updated values of the design variables.
- (10) The optimization procedure is repeated starting from step (6) until the corresponding composite objective function  $F_m$  is less than a prespecified value. If the dimension of any hole becomes less than a prespecified value, the hole is explicitly eliminated from further optimization. If the optimization procedure reaches a local minimum, the objective function formulation is automatically changed from Eq. 2 to Eq. 3 while continuing optimization starting with step (6).

### Nondestructive detection of voids

This same methodology and the accompanying software have been adapted to nondestructive determination of the actual number, sizes, shapes, and locations of possible voids inside an arbitrarily shaped solid object which can contain regions with different thermal diffusivities. If the voids are assumed to be free of any material (vacuum voids) then the only heat transfer mode across the voids is by pure thermal radiation. Thus, the thermal boundary condition on the surfaces of the voids should be of a Neumann type in terms of the fourth power of temperature. Nevertheless, since the actual void shapes and their surface radiative properties are not known *a priori*, we have decided to treat the surface of each void as an adiabatic boundary. That is, normal derivative of temperature on the surface of each void was set to zero.

A rudimentary example of a well-posed elliptic problem can now be formulated for the object of a known and fixed size and shape by providing measured temperatures  $T_{out}^m$  along the outer surface of the body, while at the same time specifying zero temperature gradient normal to the surfaces (walls) of the voids inside the solid object. Laplace's equation can now be integrated numerically in this multiply connected domain subject to measured Dirichlet boundary condition on the outer surface and the specified Neumann boundary conditions on the surfaces of the guessed voids. Nevertheless, the actual number, sizes, locations, and shapes of the voids are still unknown. Therefore, in addition to the measured values of the outer surface temperatures  $T_{out}^m$  we also need to provide measured outer surface heat fluxes  $q_{out}^m$ . This combination of  $T_{out}^m$  and  $q_{out}^m$  represents an over-specified elliptic problem meaning that in general Laplace's equation has no solution subject to these conditions, except, possibly for a very special combination of the number, sizes, locations, and shapes of the voids. Starting with a large number of guessed voids, all non-existent voids should be eliminated when their sizes reduce below a prespecified minimal value. The optimization algorithm for detection of possible voids then follows the protocol used in the inverse design of coolant flow passages.

### Results for inverse design

To demonstrate the accuracy and efficiency of the analysis and optimization algorithms a circular coated disk made of a thermally homogeneous material was assigned a constant temperature on its outer boundary and another constant temperature on a centrally located circular hole perimeter. The heat flux on the outer boundary is thus constant and analytically known. Pretending that we do not know the actual number of the holes, their sizes and shapes, we have guessed that there are three circular holes (Fig. 1) asymmetrically positioned [6] within the inner disk each having its surface temperature equal to the temperature that a single centrally located hole had. In only nine iteration cycles, requiring 1162 calls to the boundary element analysis

code, two out of three initially guessed holes have reduced to a negligible size (Fig. 1), while the third hole converged to the correct solution of a large centrally located hole. The inverse design concept was then applied with confidence to the same coated disk with ten initially guessed holes [6] all having the same surface temperature corresponding to the only correct solution of a centrally located large hole. After successfully circumventing problems with local minimas by automatically alternating between the two formulations (Eqs.(1) and (2)) for the objective function, nine holes reduced to a negligible size while the tenth hole assumed the only correct centrally located size (Fig. 2). The inverse design was then tested with general Lamé (superelliptic shapes) where three initially guessed holes had elliptic, rectangular and square shape, respectively. Each hole had the same constant surface temperature assigned that corresponded to the only correct temperature on a centrally located circular large hole. The convergence history of this test case (Figs. 3 and 4) indicate that it took over 120 optimization cycles to eliminate the initially elliptical hole and the initially square hole and to transform the initially rectangular hole into the correctly sized and centrally located circular hole.

#### Results for nondestructive detection of voids and cracks

Again, to test the accuracy of the basic analysis code and the optimization algorithm we chose the circular coated disk with a centrally located circular hole. Ratio of thermal diffusivities of the coating and the core material was 1:5. Outer surface and interface between the coating and the core material were discretized with 36 panels each. The correct solution was a centrally located circular hole that had zero surface heat flux, while the outer surface of the disk had variable temperature distribution. This time we guessed that there is one elliptically shaped void eccentrically located in the disk and that it has zero surface heat flux. The surface of the void was discretized with 16 panels. This initial guess converged (Figs. 5 and 6) to the correct centrally located circular hole solution in ten optimization cycles requiring 375 calls to the analysis code. During this exercise we varied five out of six design variables associated with Lamé curve formulation. Lamé exponent was kept at the value  $n = 2$ .

To test the capability of the code to detect proper number, sizes, shapes and locations of the possible voids, we took the same coated disk configuration but now with a narrow vertical straight crack having zero surface heat flux and placed to the right of the center of the disk as the correct solution. Outside variable temperature boundary condition was the same as in the previous case. We have decided to guess that there are three straight parallel cracks (Fig. 7), one of which corresponded with the correct crack size, shape and location. Each of the initially guessed cracks had zero surface heat flux assigned. During the optimization, the crack geometric parameters corresponding to a general Lamé curve formulation were varied except for the minor semi-axis  $b$  and for the Lamé exponent,  $n$ . Although the coating acted as an effective smoothing device for temperature gradients inside the core material, this test case converged

after 18 optimization cycles requiring 252 calls to the analysis code. The left-of-center crack and the centrally located crack reduced in size to zero (Fig.8). Thus, the capability of the code to detect thin simple cracks has been verified.

### References

1. Kennon, S.R., and Dulikravich, G.S.: The Inverse Design of Internally Cooled Turbine Blades, *ASME Journal of Engineering Gas Turbines and Power*, (Jan. 1985) 123-126.
2. Kennon, S.R. and Dulikravich, G.S.: Inverse Design of Multiholed Internally Cooled Turbine Blades," *Int. Jour. of Numerical Methods in Eng.*, Vol. 22, (1986a) 363-375.
3. Kennon, S.R. and Dulikravich, G.S.: Inverse Design of Coolant Flow Passage Shapes With Partially Fixed Internal Geometries, *International Journal of Turbo & Jet Engines*, Vol. 3, 1, (1986b) 13-20.
4. Chiang, T.L. and Dulikravich, G.S.: Inverse Design of Composite Turbine Blade Circular Coolant Flow Passages, *ASME Journal of Turbomachinery*, Vol. 108 (1986) 275-282.
5. Dulikravich, G.S.: Inverse Design and Active Control Concepts in Strong Unsteady Heat Conduction, *Applied Mechanics Reviews*, Vol. 41, No. 6 (June 1988) 270-277.
6. Dulikravich, G.S. and Kosovic, B.: Minimization of the Number of Cooling Holes in Internally Cooled Turbine Blades, ASME paper 91-GT-103, ASME Gas Turbine Conf., Orlando, FL, (June 1991); also to appear in *Int. J. of Turbo & Jet Engines*, (1992).
7. Dulikravich, G.S.: Inverse Design of Proper Number, Shapes, Sizes and Locations of Coolant Flow Passages, Proc. 10th Annual Workshop on CFD Appl., NASA MSFC, Huntsville, AL, (April 1992).
8. Dulikravich, G.S. and Martin, T.J.: Determination of the Proper Number, Locations, Sizes and Shapes of Superelliptic Coolant Flow Passages in Turbine Blades, Proc. of ICHMT Internat. Symp. on Heat Trans. in Turbomachin., Athens, Greece (Aug. 1992).
9. Dulikravich, G.S. and Hayes, L.J.: Control of Surface Temperatures to Optimize Survival in Cryopreservation, Proc. of ASME WAM'88 Symp. on Comput. Meth. in Bioeng., Ed: R.L. Spilker and B.R. Simon, BED-Vol.9, (Nov.27-Dec.2, 1988) 255-265.
10. Vanderplaats, G.N.: Numerical Optimization Techniques for Engineering Design, McGraw-Hill, New York, (1984).

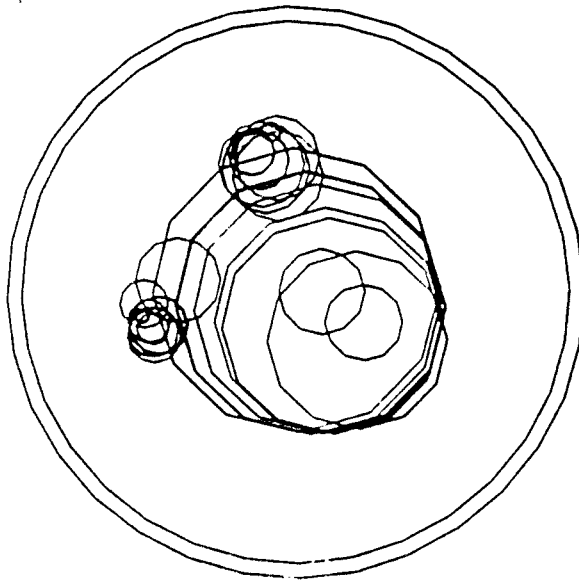


Fig. 1 Inverse design of a centrally located circular hole with an initial guess consisting of three asymmetrically positioned circular holes: configuration evolution history.

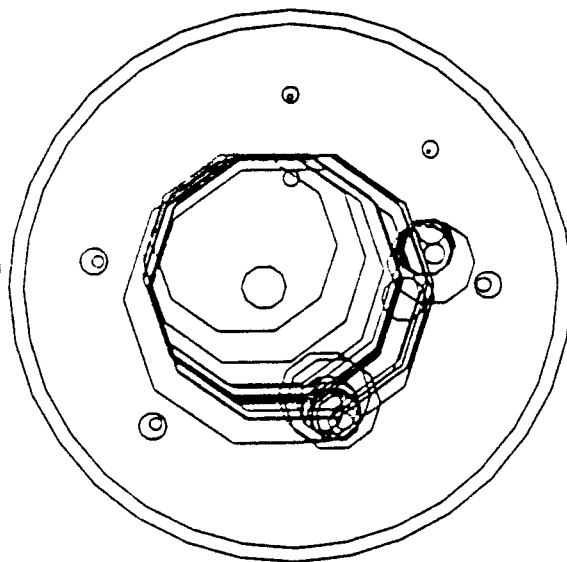


Fig. 2 Inverse design of a centrally located circular hole with an initial guess consisting of ten asymmetrically positioned circular holes: configuration evolution history.

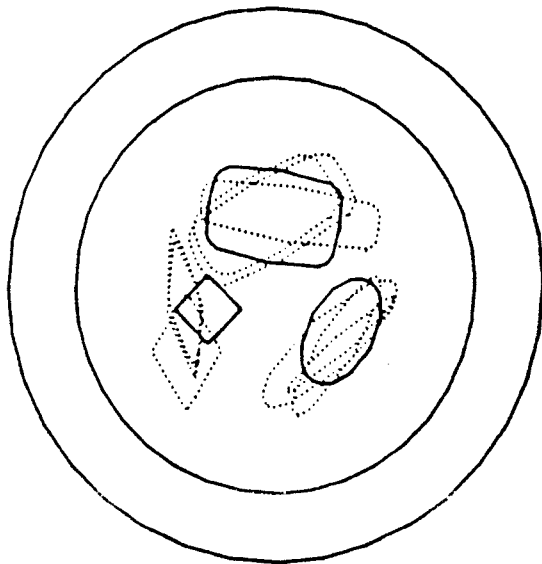


Fig. 3 Inverse design of a centrally located circular hole with an initial guess of three Lamé-type holes: first 64 optimization cycles.

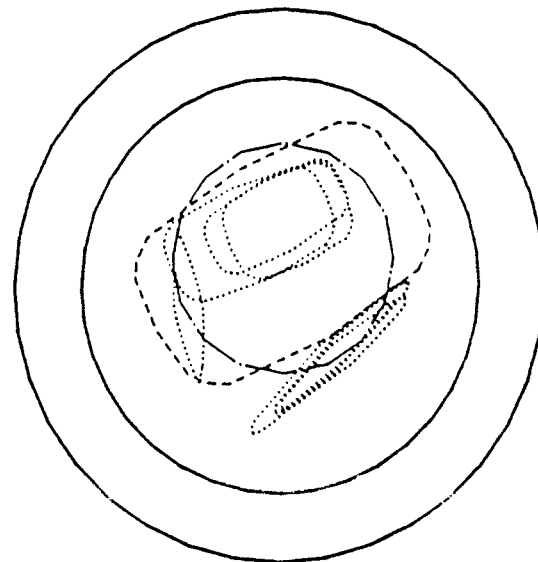


Fig. 4 Inverse design of a centrally located circular hole with an initial guess of three Lamé-type holes: optimization cycles 65-120.

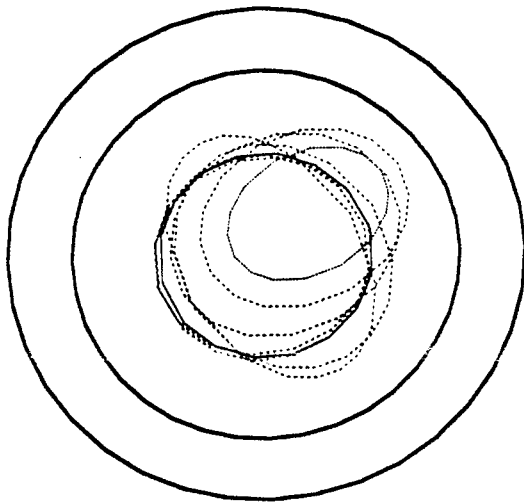


Fig.5 Detection of a centrally located circular void starting with an off-center Lamé-type void: evolution history.

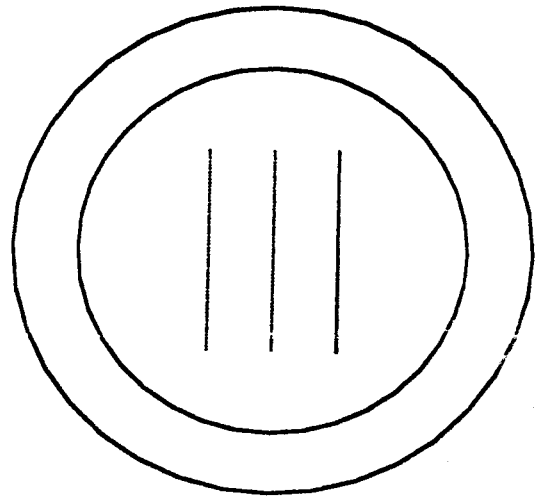


Fig.7 Detection of an off-center crack starting with three cracks belonging to a Lamé family: initial and final configuration.

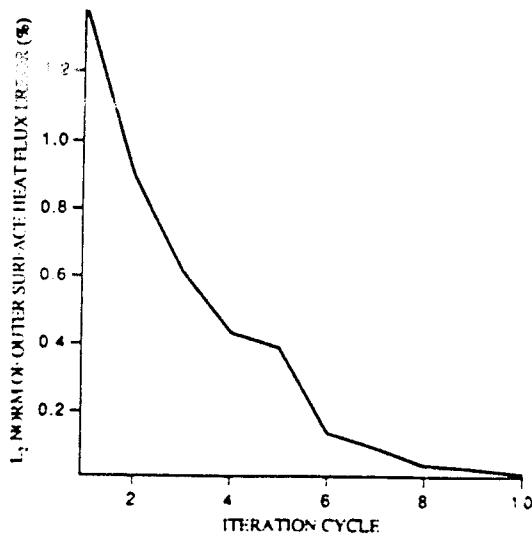


Fig.6 Detection of a centrally located circular void starting with an off-center Lamé-type void: convergence history.

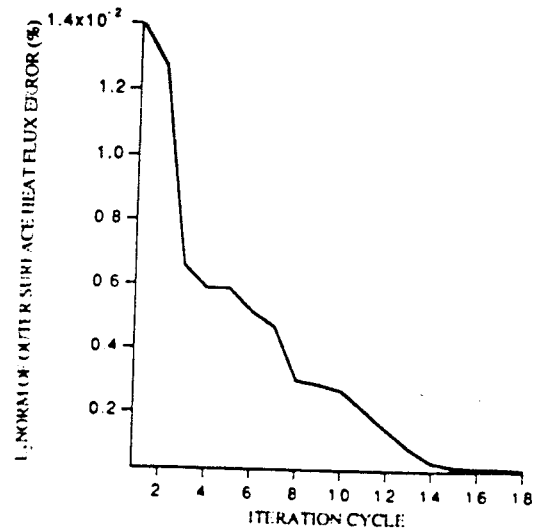


Fig.8 Detection of an off-center crack starting with three cracks belonging to a Lamé family: convergence history.



International Union of Theoretical  
and Applied Mechanics

M. Tanaka, H. D. Bui (Eds.)

# **Inverse Problems in Engineering Mechanics**

IUTAM Symposium Tokyo, 1992

Springer-Verlag

Berlin Heidelberg New York

London Paris Tokyo

Hong Kong Barcelona Budapest